ELSEVIER

Chemistry & Biology 8 (2001) 661–671

Chemistry & Biology

www.elsevier.com/locate/chembiol

Research Paper

Filamentous bacteriophage stability in non-aqueous media

Linus Olofsson, Jonas Ankarloo, Per Ola Andersson, Ian A. Nicholls*

Bioorganic and Biophysical Chemistry Laboratory, Department of Chemistry and Biomedical Sciences, University of Kalmar, SE-391 82 Kalmar, Sweden

Received 7 February 2001; revisions requested 30 March 2001; revisions received 12 April 2001; accepted 27 April 2001
First published online 21 May 2001

Abstract

Background: Filamentous bacteriophage are used as general cloning vectors as well as phage display vectors in order to study ligand–receptor interactions. Exposure to biphasic chloroform–water interface leads to specific contraction of phage, to non-infective I- or S-forms.

Results: Upon exposure, phage were inactivated (non-infective) at methanol, ethanol and 1-propanol concentrations inversely dependent upon alcohol hydrophobicity. Infectivity loss of phage at certain concentrations of 1-propanol or ethanol coincided with changes in the spectral properties of the f1 virion in ultraviolet fluorescence and circular dichroism studies.

Conclusions: The alcohols inactivate filamentous phage by a *general* mechanism – solvation of coat protein – thereby disrupting the capsid in a manner quite different from the previously reported I- and S-forms. The infectivity retention of phagemid pG8H6 in 99% acetonitrile and the relatively high general solvent resistance of the phage strains studied here open up the possibility of employing phage display in non-aqueous media.

Keywords: Organic solvent; Capsid chemistry; Circular dichroism; Fluorescence; Bacteriophage

1. Introduction

Filamentous bacteriophage (Inoviridae) infect several Gram-negative bacteria, e.g. *Escherichia coli*, *Pseudomonas* and *Xanthomonas*, in a persistent fashion. Virions are assembled at the plasma membrane and extruded through both host cell membranes without cell lysis. Filamentous coliphages have been used extensively as general cloning vectors [1,2], as well as phage display vectors [3], displaying foreign oligopeptides or proteins in fusion with a phage coat protein (for comprehensive reviews, see [4–6]).

The filamentous phage capsid is an elongated (~7 by ~700–2000 nm; strain-dependent) hollow protein tube consisting of five different proteins, the dominant by far being g8p which is present in about 2700 copies/capsid. The single-stranded phage DNA is bound and packed inside the capsid by g8p in a sequence-independent manner. The length of the resulting virion is dependent on DNA length, allowing large heterologous inserts in the phage DNA. Filamentous bacteriophage demonstrate great physical stability, being infective after exposure to high temperatures [7] or certain organic solvents [8,9].

Structures of whole filamentous phage virions, as well as solubilised coat protein, have been studied by several spectroscopic techniques. Fibre X-ray diffraction [10–12] and nuclear magnetic resonance (NMR) [13,14] studies suggest that the g8p subunits are arranged in a gently curved α-helical structure, roughly aligned with the virion axis in a five-fold rotational and approximately two-fold screw axis symmetry. Each g8p molecule makes side chain contact with 10 neighbours. The acidic N-terminus of g8p is solvent-exposed and flexible, while the hydrophobic central portion is largely buried in the capsid. In class I filamentous bacteriophage, e.g. Ff (f1, fd, M13) and IKe, g8p subunits associate with the negatively charged phosphate groups of the single-stranded phage DNA through four C-terminal lysine (IKe, also arginine) side chains in a charge density-dependent manner, so that mutation of one of the lysines gives rise to elongated virions with no apparent changes in g8p–g8p packing, as judged by fibre X-ray diffraction [12,15,16]. In these phage, the ssDNA is further stabilised by stacking interactions between bases protruding towards the filament axis [17,18]. The angle of the individual g8p subunits to the virion axis has been determined to be 13–20° by Raman spectroscopy

Abbreviations: CD, circular dichroism; ID_{50}, dose (of solvent) inactivating 50% of the colony forming or transducing units; SDS, sodium dodecyl sulphate

* Correspondence: Ian A. Nicholls;
E-mail: ian.nicholls@hik.se

1074-5521/01/$ – see front matter
PII: S1074-5521(01)00041-2

[19]. The orientation of individual g8p side chains, notably Trp_{26} [20], and side chain interactions between g8p subunits [21] have been further refined using this technique. Circular dichroism (CD) spectroscopy has previously been used to study filamentous phage secondary structure, and Pf1 virions have been determined to contain ~80% [22] to almost 100% [23] α-helix; Ff and IKe are also α-helical to a similar degree [22,24–26].

Isolated g8p solubilised in detergent micelles has a different structure than g8p in the virion. NMR determinations of M13 g8p structure in sodium dodecyl sulphate (SDS) [27] or dodecylphosphocholine [28] show a longer, hydrophobic C-terminal α-helix (residues 25–45) buried in the hydrophobic micelle interior and a shorter, amphipathic N-terminal helix (residues 8–16) perpendicular to the micelle surface; these two helices are connected by a short, flexible spacer or hinge. The L-formed structure of g8p in micelles is thought to resemble the orientation of g8p in the host plasma membrane prior to phage assembly [29]. The flexibility of the hinge, and the relative mobility of the amphipathic helix, allows the transition of g8p between the membrane-bound and virion-bound form [30,31]. IKe g8p possesses a similar L-shaped structure in myristoyllysophosphatidylglycerol micelles [32]. It has previously been postulated that virion-bound g8p is solubilised by low concentrations of SDS (0.07%), and that the process triggers a concomitant disruption of the virion in an all-or-none fashion [33].

In an earlier study, the *Pseudomonas*-specific filamentous phage Pf1 was shown to be inactivated by 50% diethyl ether, acetone, chloroform or methanol (10 min exposure, room temperature), whereas fd retained full infectivity in all the above solvents except chloroform [8]. Exposure of Ff to the chloroform–water interface at low temperatures (2°C) leads to contraction of the virion (phage filament) into a shortened, compact rod (I-form). Exposure of the filament or the I-form to the chloroform–water interface at higher temperatures (15°C or higher) further contracts the particle into a protein sphere with approximately two thirds of the phage DNA protruding and the hairpin packing initiation structure and phage origin of replication initiation specifically buried within the altered capsid (spheroid or S-form) [34]. Both the I- and S-forms are non-infectious [34] and detergent-sensitive [34,35]. The stepwise contractions of the filament to I- and S-forms have been proposed to mimic the in vivo process of unpacking the phage DNA at the host cytoplasmic membrane and depositioning g8p subunits in the membrane [36,37]. The isolation of relatively chloroform-resistant g8p mutants of fd and M13, and localisation of these mutations to discrete ring-formed bands occurring throughout the virion [11,38], implies that chloroform acts specifically, more on certain structural features in the virion than on others, as may the contact with the cytoplasmic membrane bilayer [39]. The solvent accessibility of the single tryptophan, Trp_{26}, in g8p of phage fd, has been studied in intact virions, I- and S-forms by UV spectroscopy [40]. Trp_{26} fluorescence was quenched efficiently in I- and S-forms by the apolar quenchers chloroform and trichloroethanol, but not by the more polar acrylamide, which penetrates the hydrophobic g8p–g8p interface poorly. This indicates protection from solvent of Trp_{26} in I- and S-forms, despite altered intersubunit packing [40]. In contrast to these effects of biphasic organic solvent–water systems, relatively little is known about the mechanisms involved in *water-miscible* organic solvents' inactivation of filamentous phage.

Phagemid vector pG8H6 was constructed to increase the enrichment for ligand binding clones containing bacterial receptor-derived inserts binding to e.g. IgG, fibrinogen or fibronectin [41]. We wanted to investigate this vector as a model for possible phage display applications in non-biological media. A filamentous helper phage, such as the f1-derived R408 [42], is required for the packing of pG8H6 ssDNA into infective virions (these will be referred to as 'phage' in the text, although they are really pG8H6 (Amp^R)-transducing particles). The g8p gene present in pG8H6 originates from R408 [41] and incorporation of the pG8H6-expressed g8p in pG8H6 virions should not lead to different capsid composition in pG8H6 or R408, even if the latter is prepared as a pure lysate. It should be noted that expression of g8p from pG8H6 is probably very low, due to a frameshift between the promoter and the g8p gene [41]. Thus, the nature of individual coat protein interactions should in practice be identical in pG8H6 and R408 virions. Wild-type f1, which was used in all spectroscopic studies and as a source for g8p purification, is identical to R408 in respect to the capsid, but yields higher titres due to a higher packing efficiency compared to R408 [42]. The N-pilus-specific filamentous phage IKe [43] is 55% identical to F-pilus-specific Ff in overall DNA sequence, to a lesser amount in genes encoding capsid proteins; IKe g8p has a less hydrophobic middle region, especially C-terminally of its single tryptophan Trp_{29} [44].

We present a systematic study of the influence of alcohols or aprotic organic solvents on infectivity (pG8H6, R408, IKe), as well as whole virion and isolated g8p structure (f1). One of the phage strains (pG8H6) was found to be infective after exposure to 99% acetonitrile, and also showed a significant enhancement of infectivity at intermediate alcohol concentrations. Fluorescence and CD spectroscopy of f1 virions as well as isolated f1 g8p was performed in alcohols but in the absence of detergent. Infectivity losses in relatively apolar alcohol (methanol, ethanol, 1-propanol)–water mixtures coincide with fluorescence emission λ_{max} red shifts as well as increased g8p Trp_{26} accessibility to a polar quenching agent (acrylamide). This indicates that the loss of infectivity is due to the dissolution of the virion by the alcohol, rather than specific structural changes such as the induction of I- and S-forms, is the mechanism. The apparent ID_{50} alcohol

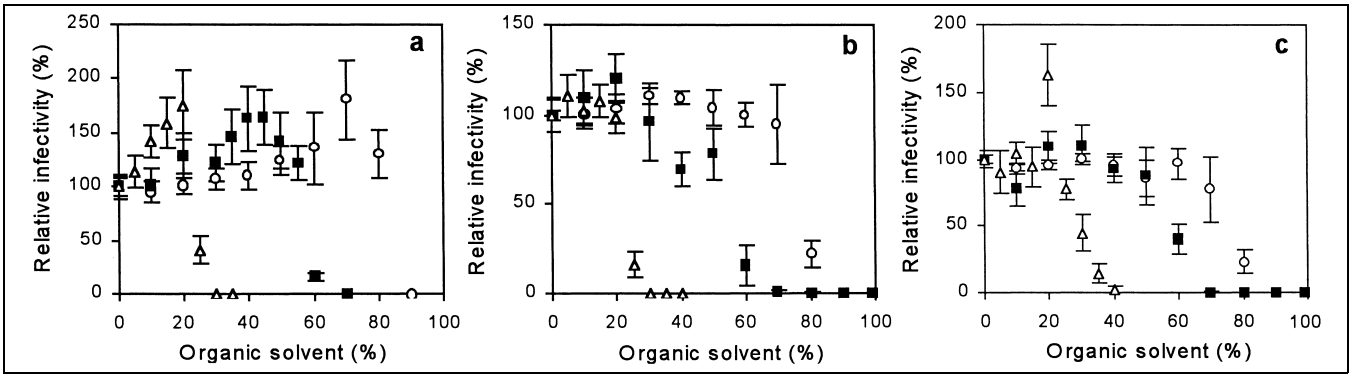

Fig. 1. Relative infectivity of (a) pG8H6, (b) R408 and (c) IKe exposed to methanol (circles), ethanol (filled squares) or 1-propanol (triangles) in 50 mM sodium phosphate, pH 7.0. Error bars represent 95% confidence intervals from nine replicates. Note different scales on *y*-axes.

concentrations correlate inversely with the hydrophobicity of the alcohol employed. CD spectroscopy indicates an α-helix to β-sheet transition at inactivating ethanol concentrations, in virions but not in isolated g8p.

2. Results

2.1. Infectivity of solvent-exposed phage

Following exposure to water-miscible organic solvents, all phage tested (pG8H6, R408, IKe) show similar tolerance curves as judged by their ability to infect indicator bacteria. Firstly, methanol, ethanol and 1-propanol inactivate the phage at concentrations inversely dependent upon alcohol hydrophobicity (Fig. 1). pG8H6 retains full infectivity at slightly higher methanol concentrations (80%) than R408 or IKe. Also, pG8H6 shows a statistically significant ($P < 0.05$) increase in infectivity after exposure to 15–20% 1-propanol, 40–45% ethanol or 70% methanol (Fig. 1a), as does IKe after exposure to 20% 1-propanol (Fig. 1c). The infectivity of all three phage is reduced at higher acetonitrile concentrations, although pG8H6 remains infective even at 99% acetonitrile (Fig. 2a). In contrast, 70% *N*,*N*-dimethylformamide inactivates pG8H6 and R408 whereas IKe remains partly infective (Fig. 2c). Prolonged exposure (24 h) of pG8H6 to 40% ethanol produces no significant difference in infectivity, relative to buffer-exposed phage (results not shown).

2.2. Solvent and pH effects

pG8H6 was exposed to 50 mM sodium phosphate (pH range 5.0–9.0) containing methanol, ethanol or propanol as described above. Tolerance curves for all alcohols are very similar to those reported in Fig. 1a (pH 7.0), except there are no apparent enhancements of infectivity at intermediate alcohol concentrations at any pH tested other than pH 7.0. Moreover, infectivity remains constant in aqueous buffer in the pH range of 5.0–9.0 (results not shown).

2.3. Solvent and temperature effects

The combined effect of ethanol and elevated temperature on pG8H6 infectivity was examined: pG8H6 was exposed to 50 mM sodium phosphate, pH 7.0 with and without 50% ethanol at different temperatures as described above. pG8H6 infectivity in 50% ethanol is significantly lowered (compared to buffer-exposed phage) at 30°C and above. Infectivity is abolished after exposure to 50% ethanol at 50°C (results not shown).

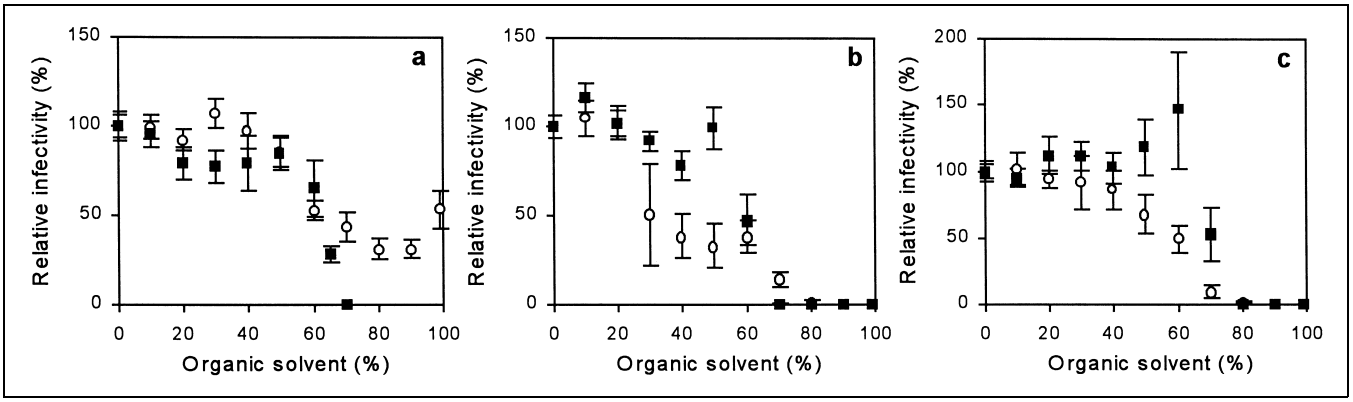

Fig. 2. Relative infectivity of (a) pG8H6, (b) R408 and (c) IKe exposed to acetonitrile (circles) or *N*,*N*-dimethylformamide (filled squares) in 50 mM sodium phosphate, pH 7.0. Error bars represent 95% confidence intervals from nine replicates. Note different scales on *y*-axes.

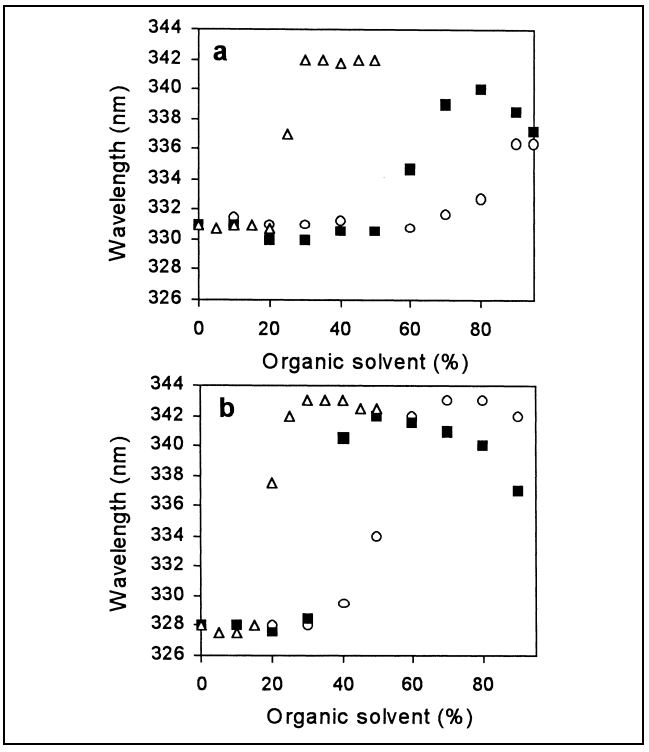

Fig. 3. Fluorescence emission maxima for (a) f1 and (b) g8p exposed to methanol (circles), ethanol (filled squares) or 1-propanol (triangles) in H_2O.

2.4. UV fluorescence spectra

The fluorescence emission spectrum of phage f1 in H_2O shows a maximum (λ_{max}) at 331 nm (Fig. 3a), in agreement with that previously reported for fd, 332 nm [45]. No significant shift in λ_{max} of f1 occurs in 0–70% methanol, 0–50% ethanol or 0–20% 1-propanol. Upon exposure to methanol (80%), ethanol (60%) or 1-propanol (25%), there is a slight red shift of λ_{max} which is fully evolved at higher concentrations of methanol (90%), ethanol (70%) or 1-propanol (30%). At extreme (90–95%) ethanol concentrations, λ_{max} blue shifts by a few nm. Purified g8p exhibits a λ_{max} of 328 nm in H_2O, which remains practically constant in up to 15% 1-propanol, 30% ethanol or 40% methanol (Fig. 3b). As in the case of f1 virions, λ_{max} is red shifted at high alcohol concentrations (60% methanol, 50% ethanol, 25% 1-propanol). The red shifts are of slightly greater magnitude than in the case of f1 and blue shifts are again apparent at extremely high alcohol concentrations. The UV *absorption* maxima of f1 or g8p do not change in any of the alcohol concentrations employed (results not shown). The plating efficiency of f1 is 0.7, in accordance with earlier reported values (0.6–0.8) for CsCl-purified fd [46].

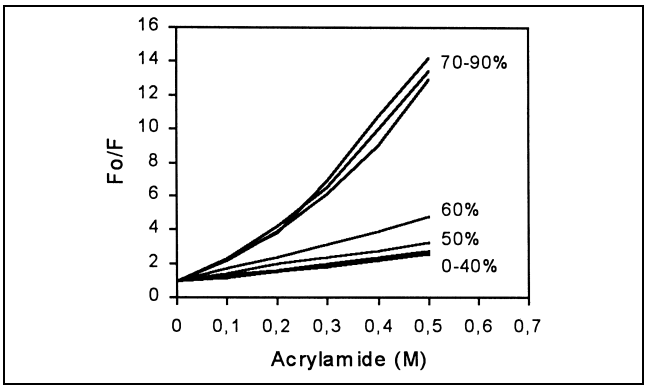

Fig. 4. Fluorescence quenching by acrylamide of Trp_{26} of f1 in ethanol/water. Ethanol content is indicated by percentages in the figure. Trp_{26} fluorescence in H_2O (F_0), divided by fluorescence at λ_{max} for the respective ethanol concentration (F), is plotted against quencher concentration, [Q]. Upward deviation of the curves at higher acrylamide concentrations indicates fluorophore–quencher complex formation.

Table 1
Quenching of Trp_{26} fluorescence by acrylamide

		PrOH (%)													
		0	5	10	15	20	25	30	35	40	50	60	70	80	90
f1	K_{sv}	3.1	2.9	2.7	2.9	2.8	6.2	10.4	9.1	8.6	8.5	5.5	7.8	8.5	9.0
	V	0	0	0	0	0	0	1.1	1.3	1.6	1.7	2.5	1.7	1.6	1.0
g8p	K_{sv}	2.6	2.5	2.4	2.4	2.9	9.2	6.9	10.6	11.8	7.7	7.7	7.9	7.8	
	V	0	0	0	0	0	1.5	1.8	1.3	1.3	1.8	1.7	1.8	2.0	
		EtOH (%)													
		0	10	20	30	40	50	60	70	80	90				
f1	K_{sv}	3.0	2.8	3.1	3.3	3.3	4.7	7.1	10.7	10.6	8.5				
	V	0	0	0	0	0	0	0	1.5	1.7	1.8				
g8p	K_{sv}	2.6	2.4	2.6	2.6	5.1	11.1	11.7	10.1	7.4					
	V	0	0	0	0	0	1.4	1.7	1.7	2.0					

Acrylamide (0–0.5 M final concentration) was added to f1 or purified g8p pre-incubated in H_2O. Fluorescence in the absence of acrylamide/fluorescence in the presence of acrylamide (F_0/F), at λ_{max} for each alcohol concentration, was plotted against acrylamide concentration (Stern–Volmer plot, see Fig. 4). Dynamic quenching constants K_{sv} and static quenching constants V were extracted from the plots using Eq. 1. In cases of $V < 0.5$, the plots were considered essentially linear and V was set at 0. K_{sv} values were then determined using the simplified linear equation (Eq. 2), which fits the tangents of the curves at 0 M acrylamide.

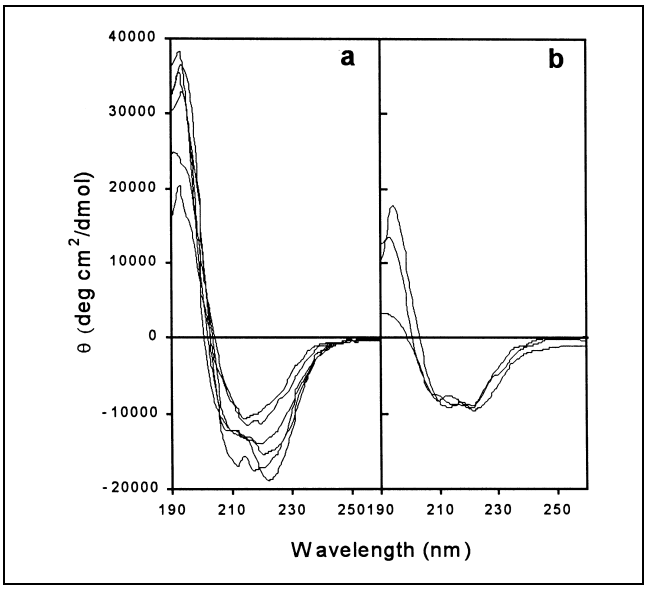

Fig. 5. CD spectra of (a) f1 and (b) g8p in ethanol/water. In a, the spectra are, from most to least negative ellipticity at 222 nm, f1 in H_2O, 95%, 60%, 90%, 80% and 70% ethanol respectively. In b, the spectra are, from most to least negative ellipticity at 230 nm, g8p in H_2O, 80% and 50% ethanol, respectively.

2.5. *UV fluorescence quenching*

Fig. 4 provides a typical example of acrylamide quenching the Trp_{26} of f1, revealing a substantial increase in K_{sv} values at higher ethanol concentrations. As shown in Table 1, K_{sv} for phage f1 in H_2O is 3.0–3.1, which does not change significantly in up to 40% ethanol or up to 20% 1-propanol. K_{sv} increases in 50–60% ethanol and 25% 1-propanol, reaching a plateau at higher alcohol concentrations. In addition, static quenching is evident at ethanol concentrations of 70% and above, and at 1-propanol concentrations of 30% and above, indicated by an upward deviation from linearity (Fig. 4). At 90% ethanol, K_{sv} decreases slightly. Purified g8p in H_2O and up to 30% ethanol shows a K_{sv} of 2.6 (Table 1), increasing in 40% and reaching a maximum in 50–70% ethanol, where static quenching can also be observed. In 0–20% 1-propanol, K_{sv} is low (2.6–2.9) but it rises sharply to 9.2 in 25% 1-propanol, at and above this concentration static quenching also occurs. Maximal K_{sv} in ethanol and 1-propanol is higher for g8p than for f1.

2.6. *CD*

When exposed to ethanol concentrations ranging from 0 to 50% in H_2O, f1 yields CD spectra nearly identical in terms of shape and ellipticity magnitude, indicating no change in α-helix content (Fig. 5a). A decrease in negative ellipticity at 222 nm is observed for f1 in 60% ethanol. Upon exposure to 70% ethanol, there is a decrease in the magnitude of ellipticity at both 208 and 222 nm, and a decrease in positive ellipticity at 192 nm. This indicates a substantial loss of α-helix as well as an increase in β-sheet content, notably in the anti-parallel conformation as confirmed by calculations using the CD spectrum deconvolution program CDNN (not shown). In the case of purified g8p, there are no apparent differences above 200 nm between the CD spectra in H_2O and up to 80% ethanol. However, at 192 nm, there is an increase in positive ellipticity as ethanol concentrations increase (Fig. 5b).

3. Discussion

3.1. *Infectivity after solvent exposure*

The results indicate that the alcohol inactivation of filamentous phage in this study is caused by decreased overall solvent polarity, weakening the hydrophobic inter-g8p forces stabilising the phage filament. The more hydrophobic the alcohol, the lower the concentration needed for inactivating the phage (Fig. 1). This confirms the view that hydrophobic interactions between filamentous phage coat proteins make a significant contribution to the stability of this type of virion [44]. With the exception of pG8H6 in acetonitrile (Fig. 2a), all three phage show similar tolerances to acetonitrile or *N*,*N*-dimethylformamide. IKe also exhibits alcohol tolerance similar to pG8H6 and R408, despite the differences in g8p. This points to the generality of the molecular basis for structural and functional stability of filamentous bacteriophage, and also suggests that the inactivation of Ff-derived phage (pG8H6, R408) and IKe observed in this study relies on the same mechanism. The inactivation could be due to gross rearrangements of coat protein within the capsid, as earlier described for I- and S-forms [8,34]; or coat protein could be solvated and completely separated from the virion. This question was addressed in the following spectroscopic studies.

3.2. *Temperature and solvent effects on infectivity*

While fully retaining infectivity in 50% ethanol at 20°C (Fig. 1a), pG8H6 significantly loses infectivity in 50% ethanol at only moderately elevated temperatures (30°C and above). This is in contrast to the high stability of filamentous bacteriophage at either high temperatures [7] or 50% ethanol (Fig. 1). Weakening of the hydrophobic g8p–g8p interactions by ethanol may render the virion hypersensitive to temperature due to thermal disruption of the electrostatic forces between g8p and DNA, assuming the latter are quite weak. These combined effects seem to overcome the simultaneous temperature-induced increase in g8p–g8p interaction strength as well as the strengthened g8p–DNA interaction due to lowered solvent polarity.

3.3. UV fluorescence spectroscopy; f1

The emission λ_{max} of f1 is 331 nm, which is indicative of the Trp_{26} being buried in a highly hydrophobic milieu. For comparison, phage IKe has a λ_{max} of 337 nm due to its more polar region surrounding Trp_{29} [26]. An increase in the polarity of the environment surrounding the fluorophore, in this case the indole ring of the single tryptophan (Trp_{26}) of g8p, causes a red shift of the fluorescence spectrum due to increased energy loss from the excited fluorophore to reorienting solvent dipoles and neighbouring amino acids [47]. Exposure of f1 to 1-propanol (0–20%), ethanol (0–50%) or methanol (0–60%, Fig. 3a), causes no significant change in f1 λ_{max}. This indicates that the local environment of g8p is constant over these concentration ranges and implies that the g8p–g8p hydrophobic interactions are not perturbed. The intermediate red shifts of f1 in 1-propanol (25%), ethanol (60%) or methanol (80%) suggest that a fraction of the phage population is disrupted. The fully evolved red shifts of f1 emission λ_{max} from 331 nm (H_2O) to 339 nm (ethanol, 70%) or 342 nm (1-propanol, 30%) are concomitant with infectivity loss of R408 at 70% ethanol and 30% 1-propanol (Fig. 1b). It should be noted that despite the fact that the virion is diluted 100-fold in buffer after exposure to a solvent (in the infectivity study), the sudden changes in infectivity as a function of solvent polarity coincide with the points where changes in spectral properties are observed, despite the fact that spectra are recorded in the organic solvent concerned. This implies that the changes induced in the virion structure responsible for the loss of infectivity are non-reversible within this time frame. At even higher alcohol concentrations, f1 λ_{max} is shifted to a lower wavelength (blue shift) due to the already exposed Trp_{26} being present in a gradually more non-polar solvent. This indicates complete disruption of the phage structure separating the capsid proteins from the DNA as well as from each other and exposing Trp_{26} freely to the solvent. However, fluorescence quenching by acrylamide was investigated to exclude the alternative explanation of g8p subunit rearrangement within the capsid being responsible for the fluorescence red shifts.

3.4. Fluorescence quenching; f1

The increase of K_{sv} is due to a decrease in fluorescence intensity caused by enhanced collision rate between the quencher (acrylamide) and the excited indole ring of Trp_{26}. Exposure of f1 to 1-propanol (0–20%), ethanol (0–50%) or methanol (0–60%) causes no significant alteration in K_{sv}, indicating Trp_{26} to be equally and minimally accessible to acrylamide. The slightly increased K_{sv} values for f1 at 50% ethanol or 25% 1-propanol suggest a rise in the fraction of disrupted phage causing an increased exposure of Trp_{26} in g8p to the quencher. The significantly increased K_{sv} values for f1 at 70% ethanol or 30% 1-propanol, well in agreement with infectivity data (Fig. 1b) and emission λ_{max} shifts (Fig. 3a), suggest almost total accessibility of Trp_{26} to the quencher, again indicating complete disruption of the phage structure. At these and higher alcohol concentrations (70–90% ethanol, 30–90% 1-propanol for f1), static quenching due to complex formation between Trp_{26} and acrylamide may be observed at acrylamide concentrations above 0.2 M (Fig. 4 and Table 1), as represented by upward curvature of the Stern–Volmer plots. This too indicates free accessibility of Trp_{26} to acrylamide, in contrast to the dynamic nature of the quencher–tryptophan interaction at lower alcohol concentrations where small fluctuations in the capsid g8p array may allow acrylamide only limited access to the supposedly buried Trp_{26} [48]. The fact that acrylamide does not quench chloroform-induced (non-infective but g8p-retaining) I- and S-forms [36,40] strongly suggests that 70% ethanol and 30% 1-propanol solvate g8p, leading to increased dynamic (collisional) and static (by complexation) quenching.

3.5. CD spectroscopy; f1

The CD spectrum of phage f1 in H_2O (Fig. 5a) is consistent with previously reported CD spectra of other type I filamentous bacteriophage [22,26,35,36,40], where the negative ellipticity at 222 nm is unusually large relative to the 208 nm minimum. The similarity of the CD spectra of f1 exposed to 0–50% ethanol suggests no influence from the increased solvent polarity of the surrounding media on the f1 capsid secondary structure. Nevertheless, exposure to 70% ethanol causes a substantial decrease in α-helix and an increase in β-sheet content, indicated by the single negative ellipticity minimum of 216 nm, as well as calculations with CDNN. Earlier, β-polymeric g8p aggregates have been described as artifacts from g8p preparation [24,49,50], while there is no previous report of β-polymeric g8p within any described capsid form. An anti-parallel β-sheet conformation of g8p is not likely to be compatible with g8p–DNA interactions as in intact virions, due to the presence of acidic (Asp, Glu) amino acids in the g8p N-terminus [44]. CD spectra of I- and S-forms show ellipticity minima at 208 and 222 nm [40,51]. Collectively, these observations support our theory that capsid disruption, not capsid rearrangement leading to I- and S-forms, is responsible for the infectivity loss in alcohols. The decrease in negative ellipticity at 222 nm in 60% ethanol is probably caused by a fraction of the phage population being disrupted; again here an increase in β-sheet is suggested by CDNN calculations. Interestingly, there is a trend toward increased α-helicity ranging from 80% to 95% ethanol exposure (Fig. 5a) which is most likely explained by α-helix induction analogous to that caused by trifluoroethanol [52]; ethanol is here assumed to elicit similar effects at high concentrations.

The coincidence of infectivity loss, UV fluorescent spec-

tral red shifts and β-sheet formation within narrow alcohol concentration intervals (60–70% ethanol, 25–30% 1-propanol) provides strong evidence in support of the postulate that the phage are disassembled in an all-or-none, or cooperative, fashion. Notably, neither UV fluorescence emission maxima (Fig. 3a), Trp_{26} availability to acrylamide (K_{sv}; Table 1) nor CD spectral characteristics (including the accentuated ellipticity minimum at 222 nm) change at ethanol concentrations (0–50%) below the inactivating concentration. The irreversibility of this process is illustrated in that the dilution, and subsequent incubation, of all solvent-exposed phage in sodium phosphate buffer prior to infection does not seem to reverse the inactivation. The high plating efficiency of the f1 lysate used for the spectroscopic studies excludes the possibility that a majority of these phage were inactivated by any *other* means prior to solvent-induced disassembly.

3.6. *UV fluorescence spectroscopy; purified g8p*

The red shifts of λ_{max} of isolated g8p occur at consistently lower alcohol concentrations than in f1 virions. This suggests (i) initial aggregation of g8p by hydrophobic forces, and (ii) alcohol-mediated disruption of such aggregates and exposure of Trp_{26} to the medium. These effects are again correlated with general solvent polarity. The g8p aggregates are probably more easily dissolved than the virions due to less ordered g8p–g8p packing and the absence of the additional stabilisation provided by the electrostatic g8p–ssDNA interaction present in f1 virions. The observed maximal red shift in ethanol or methanol is larger for g8p than for f1, since f1 red shifts occur at very high alcohol concentrations where the relatively apolar solvent itself introduces a blue shift of the fluorescence spectrum. It is noteworthy that the highest λ_{max} for f1 and g8p in 1-propanol (342 nm) and the λ_{max} in 80% ethanol (340 nm) are comparable, indicating similar Trp_{26} solvent accessibility.

3.7. *Fluorescence quenching; purified g8p*

Isolated g8p has a low K_{sv} (2.6) in H_2O, which is indicative of the fluorophore being in a predominantly apolar environment, and suggests that Trp_{26} is buried inside the g8p aggregates and that it is sterically shielded from the quencher. SDS micelles of fd coat protein, where the protein is monomeric [27], have earlier been reported to show a K_{sv} of 5.0 for acrylamide quenching [40]. Further support for the disruption of g8p aggregates is given by the increase in dynamic (K_{sv}), as well as the occurrence of static (V) quenching at 25% 1-propanol or 50% ethanol; in agreement with the λ_{max} red shifts.

3.8. *CD spectroscopy; purified g8p*

SDS-purified and dialysed g8p appears α-helical in both 0%, 50% and 80% ethanol, resembling earlier CD spectra of SDS-inactivated phage [33] or SDS-purified g8p [40]; thus extensive dialysis against water does not seem to affect the g8p secondary structure. The strong negative ellipticity at 222 nm in f1 (Fig. 5a, H_2O-exposed phage), attributed to ordered g8p–g8p side chain interactions in filamentous phage virions [25], is not present in g8p aggregates (Fig. 5b). This, together with the higher susceptibility of purified g8p to ethanol (Fig. 3, Table 1), points to a less ordered packing of g8p in aggregates than in virions. Suppressed positive ellipticity at 192 nm (absorptive flattening) has been assigned to shielding of some chromophores by others in large aggregates [53]; the disruption of such g8p aggregates is seen in the increase in ellipticity at 192 nm at higher ethanol concentrations (Fig. 5b).

Possible solvent effects on the phage adsorption protein g3p, which lead to altered infectivity, cannot be excluded judging from the data presented here. g3p consists of three domains, of which the N-terminal D1 and D2 domains are responsible for binding to the bacterial TolA inner membrane receptor [54] and pilus tip, respectively. Crystal structures of the g3p D1–D2 from fd [7] and M13 [55] reveal that these domains, connected to each other by a glycine-rich linker, are also in hydrophobic contact so that the TolA binding site is masked by the D2 domain. Upon binding to the pilus tip, D1 is unmasked and promotes infection by binding TolA. Conformational changes in g3p at moderately elevated temperatures (45–60°C) have been implicated in increasing pilus-*independent* infectivity more than 10-fold [7]. However, any contribution of pilus-independent infection to the apparent increase in infectivity observed in some cases in this study would most probably be several orders of magnitude too low to be observed on the F′ host used here, considering the relatively high detection limit inferred by our plating method.

4. Significance

Filamentous bacteriophage (Inoviridae) consist of single-stranded DNA surrounded by small, α-helical and highly hydrophobic capsid proteins in a helical array. The virion structure is highly stable, as filamentous phage remain infective after e.g. exposure to high temperatures. As reported earlier, filamentous phage are inactivated by a biphasic chloroform–water system through gross, specific capsid rearrangements (I- and S-capsid forms). These are thought to mimic the deposition of capsid protein in the *Escherichia coli* cytoplasmic membrane, concomitant with internalisation of phage DNA. We have exposed filamentous phage to monophasic organic solvent–water systems and report coincident loss of infectivity and shifts in virion spectral properties as studied by UV fluorescence and CD, suggesting a drastic increase in exposure of individual capsid protein subunits to solvent. We propose that the alco-

hols employed in this study influence filamentous phage by a *general* mechanism – solvation of major coat protein by weakening of hydrophobic inter-coat protein forces – thereby disrupting the capsid in a manner quite different from chloroform-induced specific contraction, where coat protein is retained. A possible additional contribution of solvent-induced changes in the F pilus attachment protein g3p remains to be investigated, as does the reason for the infectivity enhancements of the cloning vector, phagemid pG8H6 at intermediate alcohol concentrations. The infectivity retention of pG8H6 in 99% acetonitrile as well as the relatively high general solvent resistance of the phage strains studied here open up the possibility of employing phage display in non-aqueous media.

5. Materials and methods

5.1. Strains and media used for infectivity assays

Phagemid pG8H6 was grown on *E. coli* TG1/F′ on NA (Merck) ampicillin (50 μg/ml) plates overnight at 37°C. Phage R408 (Promega) was grown on *E. coli* TG1/F′ on fresh (< 1 week) 3YT (24 g tryptone (Difco), 15 g yeast extract (Merck), 5g NaCl, 12 g Bacto-agar (Oxoid)/1000 ml H_2O) plates, using modified B top agar (10 g tryptone, 8 g NaCl, 3 g Bacto-agar/1000 ml H_2O) overnight at 37°C. Phage IKe was grown on *E. coli* JE2571/N3 on fresh 2YT (16 g tryptone, 10 g yeast extract, 5 g NaCl, 12 g Bacto-agar/1000 ml H_2O) tetracycline (12.5 μg/ml) plates using modified B top agar, for 2 days at 20°C.

5.2. Plaque lysate of IKe and R408

Phage IKe or R408 was propagated as described above. 50–100 well-isolated plaques were picked with a sterile pasteur pipette and transferred to 10 ml 50 mM Na_2HPO_4/NaH_2PO_4, pH 7.0. Phage were eluted overnight at 4°C, agar was removed by centrifugation at 5000 rpm, 15°C for 15 min (Hermle 220.86 swing-out rotor) and the lysates were stored at 4°C.

5.3. Plate lysate of pG8H6

E. coli TG1/F′ (pG8H6) was grown in LB (10 g tryptone, 5 g yeast extract, 5 g NaCl/1000 ml H_2O) ampicillin (50 μg/ml) until exponential phase (3 h; $OD_{635} = 0.25$) and left at 20°C for 15 min. R408 helper phage (Promega) was added to 1 ml cells at a multiplicity of infection (MOI) = 50, and infection was continued for 15 min. The double-infected cells were plated on NA+ampicillin plates using SA (10 g tryptone, 5 g NaCl, 5 g Bacto-agar/1000 ml H_2O). After overnight incubation at 37°C, top layers were transferred to 50 ml LB and shaken for 4 h at 37°C. Cell debris and agar was removed by centrifugation at 10 000 rpm, 15°C for 20 min (Beckman JA-20 rotor), followed by filtration through a 0.22 μm sterile filter. The lysate was made up to 15% with sterile glycerol and stored at −20°C.

5.4. CsCl purification of f1

E. coli TG1/F′ (early exponential phase) in 100 ml LB was infected with f1 phage at MOI = 1. After 1 h shaking at 37°C, 1 ml of the culture was transferred to 1 L LB. The culture was shaken for 24 h at 37°C. To remove cells, the culture was centrifuged at 4700 rpm, 4°C for 10 min (Beckman JA-10 rotor), and the supernatant recentrifuged at 7500 rpm, 4°C for 10 min (JA-10). f1 was precipitated by adding 0.15 volume of PEG/NaCl (40 g PEG 6000, 46.7 g NaCl, 190 ml H_2O) to the supernatant, then stored overnight at 4°C. After centrifugation at 7500 rpm, 4°C for 10 min (JA-10), the supernatant was removed and the pellet was recentrifuged at 2000 rpm, 4°C for 20 min (JA-10) for complete removal of supernatant. The pellet was dissolved by adding 33 ml (10 mM sodium citrate, 0.1% sarcosyl NL-97, pH 7.6), reprecipitated by adding 0.3 volume of PEG/NaCl (40 g PEG 6000, 7 g NaCl, 190 ml H_2O), and stored at 4°C for 2 h. f1 was pelleted by centrifugation at 7500 rpm, 4°C for 30 min (JA-10), then resuspended in 10 ml citrate buffer (10 mM Na-citrate, pH 7.6). Phage were purified by sedimentation in a CsCl density gradient (4.7 g CsCl/10 ml f1-citrate solution) by centrifugation at 46 000 rpm, 15°C for 20 h (Beckman 70.1 Ti rotor). The phage band was collected and diluted in 10 ml citrate buffer and the resultant solution was centrifuged at 34 000 rpm, 15°C for 3.5 h (70.1 Ti). The phage-containing pellet was resuspended in H_2O and phage were stored at −20°C until further use. The f1 concentration was determined photometrically at 269 nm using an absorption coefficient of 3.84 mg^{-1} cm^2 [46]. Plating efficiency was determined by titration of f1 on *E. coli* TG1/F′ using modified B top agar, 2YT plates and incubation at 37°C overnight. The concentration of infective f1 particles was divided by the concentration of physical f1 particles as determined above, assuming an anhydrous weight of one f1 virion of 2.42×10^{-17} g [46].

5.5. Infectivity assay

10^5–10^6 plaque forming units (IKe, R408) or transducing units (pG8H6) were exposed to 50 mM Na_2HPO_4/NaH_2PO_4, pH 7.0, containing organic solvents (0–99%) for 30 min at 20°C. Exposed virions were diluted 1:100 in 50 mM Na_2HPO_4/NaH_2PO_4, pH 7.0 and incubated for 30 min. 100 μl of this dilution was added to 200 μl indicator bacteria (cultured overnight in LB, re-inoculated and grown in TB (Terrific Broth; 12 g tryptone, 24 g yeast extract, 4 ml (5.04 g) glycerol/900 ml H_2O, 100 ml separately sterilised 0.17 M KH_2PO_4, 0.72 M K_2HPO_4) until $OD_{635} = 0.25$, aliquoted at 20°C and used within 1 h). After 30 min of infection, 100 μl portions were plated as described above. Resulting plaque (IKe, R408) or transfectant colonies (pG8H6) at any given organic solvent concentration were related to the number of plaques or colonies resulting from pure buffer exposure (0% organic solvent) as a measure of relative infectivity. Each measurement was performed in triplicate and each experiment was repeated at least three times. Data were treated statistically using the unpaired *t*-test and the Mann–Whitney *U*-test.

5.6. Isolation of g8p

f1 phage (9 mg/ml) was dissociated at a final concentration of 1% (w/v) SDS, pH 5.4 on a rocking table at 37°C overnight. 200 µl dissociated phage was loaded onto a Superose 12 HR 10/30 column (Pharmacia) connected to a Perkin-Elmer 200 Ic HPLC pump. The column was eluted (0.1 ml/min) with 5 mM citric acid (pH 4.0), 50 mM Na_2SO_4, 1% SDS, and peaks were detected at 206 nm [56] on an Applied Biosystems 785A programmable absorbance detector. g8p fractions were collected and dialysed exhaustively against water in a 2000 MW cut-off dialysis tube (Spectra/Por) and concentration was determined at 280 nm using an absorption coefficient of 1.65 mg^{-1} cm^2 [24].

5.7. Intrinsic tryptophan fluorescence of f1 and g8p

f1 virions (22 µg/ml final concentration) and g8p (9 µg/ml final concentration) were exposed to alcohols (0–95% or 0–90% respectively, in H_2O), for 30 min in the dark at 20°C. Tryptophan emission spectra were recorded (290–400 nm) at 20°C with a Hitachi F-2000 fluorescence spectrophotometer at an excitation wavelength of 295 nm to minimise interference from tyrosine [48]. The excitation and emission bandpasses were set at 10 nm and the scan speed was set at 60 nm/min. Fluorescence emission maxima (λ_{max}) were extracted from the spectra and plotted against alcohol concentration.

5.8. Quenching of fluorescence of f1 and g8p

f1 virions (50 µg/ml final concentration) and g8p (70 µg/ml final concentration) were exposed to alcohols (0–90% or 0–80% in H_2O, respectively) for 30 min in the dark at 20°C, followed by immediate addition of acrylamide (0–0.5 M final concentration). Acrylamide was prepared as 8 M stock solutions in the respective organic solvent (0–90%). Tryptophan emission spectra were recorded as for tryptophan fluorescence measurements above. Trp_{26} fluorescence in the absence of acrylamide at λ_{max} for the respective alcohol concentration (F_0), divided by the fluorescence in the presence of acrylamide (F), was plotted against acrylamide concentration, [Q]. The following equation [40,47],

$$F_0/F = (1 + K_{sv}[Q])e^{V[Q]} \quad (1)$$

was fitted to the plots to extract dynamic quenching constants K_{sv} and static quenching constants V by a least-squares procedure using the KaleidaGraph for Windows software package (Synergy Software, Reading, PA, USA). In cases of V being very low (< 0.5), the plots were considered linear and the simplified equation,

$$F_0/F = 1 + K_{sv}[Q] \quad (2)$$

was used to determine K_{sv} from the linear regions of the plots (tangents at 0 M acrylamide).

5.9. CD

f1 virions (93 µg/ml final concentration) and g8p (0.11 mg/ml final concentration) were exposed to ethanol (0–95% or 0–80% in H_2O, respectively) for 30 min at 20°C. CD spectra were recorded on a CD6 spectrodichrograph (Jobin-Yvon Instruments SA, France) at 20°C with a path length of 1 mm for f1 and 5 mm for g8p. Data were collected in the wavelength range 190–260 nm at 0.5 nm intervals with an integration time of 2 s. Each spectrum, both sample and background, was the average of five (f1) or three scans (g8p), separately intercompared before summation to detect anomalous alterations during the scanning period. Difference spectra were generated by subtracting the background spectrum from the corresponding sample spectrum. Secondary structure calculations were performed using CDNN [57].

Acknowledgements

pG8H6 was a kind gift from Dr Lars Frykberg, Swedish Agricultural University, Uppsala, Sweden. IKe and *E. coli* JE2571/N3 were kind gifts from Dr Deborah A. Steege, Duke University, Durham, NC, USA. We thank Prof. Uno Carlsson, University of Linköping, Sweden, for help with CD spectroscopy, and Dr A. Michael Lindberg, University of Kalmar, Sweden, for fruitful discussions. This work was supported by grants from the Graninge Foundation, the Carl Trygger Foundation and the University of Kalmar.

References

[1] J. Vieira, J. Messing, The pUC plasmids, an M13mp7-derived system for insertion mutagenesis and sequencing with synthetic universal primers, Gene 19 (1982) 259–268.
[2] C. Yanisch-Perron, J. Vieira, J. Messing, Improved M13 phage cloning vectors and host strains: nucleotide sequences of the M13mp18 and pUC19 vectors, Gene 33 (1985) 103–119.
[3] G.P. Smith, Filamentous fusion phage: novel expression vectors that display cloned antigens on the virion surface, Science 228 (1985) 1315–1317.
[4] H.R. Hoogenboom, A.P. de Bruine, S.E. Hufton, R.M. Hoet, J.W. Arends, R.C. Roovers, Antibody phage display technology and its applications, Immunotechnology 4 (1998) 1–20.
[5] P. Forrer, S. Jung, A. Plückthun, Beyond binding: using phage display to select for structure, folding and enzymatic activity in proteins, Curr. Opin. Struct. Biol. 9 (1999) 514–520.
[6] D.J. Rodi, L. Makowski, Phage-display technology – finding a needle in a vast molecular haystack, Curr. Opin. Biotechnol. 10 (1999) 87–93.
[7] P. Holliger, L. Riechmann, R.L. Williams, Crystal structure of the two N-terminal domains of g3p from filamentous phage fd at 1.9 Å: evidence for conformational lability, J. Mol. Biol. 288 (1999) 649–657.
[8] K. Amako, K. Yasunaka, Ether induced morphological alteration of Pf-1 filamentous phage, Nature 267 (1977) 862–863.
[9] J. Berglund, C. Lindbladh, I.A. Nicholls, K. Mosbach, Selection of phage display combinatorial library peptides with affinity for a yohimbine imprinted methacrylate polymer, Anal. Commun. 35 (1998) 3–7.
[10] M.J. Glucksman, S. Bhattacharjee, L. Makowski, Three-dimensional structure of a cloning vector. X-ray diffraction studies of filamentous

bacteriophage M13 at 7 Å resolution, J. Mol. Biol. 226 (1992) 455–470.
[11] D.A. Marvin, R.D. Hale, C. Nave, M.H. Citterich, Molecular models and structural comparisons of native and mutant class I filamentous bacteriophages Ff (fd, f1, M13), If1 and IKe, J. Mol. Biol. 235 (1994) 260–286.
[12] M.F. Symmons, L.C. Welsh, C. Nave, D.A. Marvin, R.N. Perham, Matching electrostatic charge between DNA and coat protein in filamentous bacteriophage. Fibre diffraction of charge-deletion mutants, J. Mol. Biol. 245 (1995) 86–91.
[13] S.J. Opella, T.A. Cross, J.A. DiVerdi, C.F. Sturm, Nuclear magnetic resonance of the filamentous bacteriophage fd, Biophys. J. 32 (1980) 531–548.
[14] W.M. Tan, R. Jelinek, S.J. Opella, P. Malik, T.D. Terry, R.N. Perham, Effects of temperature and Y21M mutation on conformational heterogeneity of the major coat protein (pVIII) of filamentous bacteriophage fd, J. Mol. Biol. 286 (1999) 787–796.
[15] J. Greenwood, G.J. Hunter, R.N. Perham, Regulation of filamentous bacteriophage length by modification of electrostatic interactions between coat protein and DNA, J. Mol. Biol. 217 (1991) 223–227.
[16] G.J. Hunter, D.H. Rowitch, R.N. Perham, Interactions between DNA and coat protein in the structure and assembly of filamentous bacteriophage fd, Nature 327 (1987) 252–254.
[17] A. Casadevall, L.A. Day, DNA packing in the filamentous viruses fd, Xf, Pf1 and Pf3, Nucleic Acids Res. 10 (1982) 2467–2481.
[18] A. Casadevall, L.A. Day, Silver and mercury probing of deoxyribonucleic acid structures in the filamentous viruses fd, If1, IKe, Xf, Pf1, and Pf3, Biochemistry 22 (1983) 4831–4842.
[19] S.A. Overman, M. Tsuboi, G.J. Thomas Jr., Subunit orientation in the filamentous virus Ff(fd, f1, M13), J. Mol. Biol. 259 (1996) 331–336.
[20] M. Tsuboi, S.A. Overman, G.J. Thomas Jr., Orientation of tryptophan-26 in coat protein subunits of the filamentous virus Ff by polarized Raman microspectroscopy, Biochemistry 35 (1996) 10403–10410.
[21] M. Matsuno, H. Takeuchi, S.A. Overman, G.J. Thomas Jr., Orientations of tyrosines 21 and 24 in coat subunits of Ff filamentous virus: determination by Raman linear intensity difference spectroscopy and implications for subunit packing, Biophys. J. 74 (1998) 3217–3225.
[22] B.A. Clack, D.M. Gray, A CD determination of the alpha-helix contents of the coat proteins of four filamentous bacteriophages: fd, IKe, Pf1, and Pf3, Biopolymers 28 (1989) 1861–1873.
[23] L.A. Day, C.J. Marzec, S.A. Reisberg, A. Casadevall, DNA packing in filamentous bacteriophages, Annu. Rev. Biophys. Biophys. Chem. 17 (1988) 509–539.
[24] Y. Nozaki, B.K. Chamberlain, R.E. Webster, C. Tanford, Evidence for a major conformational change of coat protein in assembly of fl bacteriophage, Nature 259 (1976) 335–337.
[25] G.E. Arnold, L.A. Day, A.K. Dunker, Tryptophan contributions to the unusual circular dichroism of fd bacteriophage, Biochemistry 31 (1992) 7948–7956.
[26] K.A. Williams, C.M. Deber, Biophysical characterization of wild-type and mutant bacteriophage IKe major coat protein in the virion and in detergent micelles, Biochemistry 35 (1996) 10472–10483.
[27] C.H. Papavoine, R.N. Konings, C.W. Hilbers, F.J. van de Ven, Location of M13 coat protein in sodium dodecyl sulfate micelles as determined by NMR, Biochemistry 33 (1994) 12990–12997.
[28] C.H. Papavoine, J.M. Aelen, R.N. Konings, C.W. Hilbers, F.J. Van de Ven, NMR studies of the major coat protein of bacteriophage M13. Structural information of gVIIIp in dodecylphosphocholine micelles, Eur. J. Biochem. 232 (1995) 490–500.
[29] R.B. Spruijt, M.A. Hemminga, The in situ aggregational and conformational state of the major coat protein of bacteriophage M13 in phospholipid bilayers mimicking the inner membrane of host *Escherichia coli*, Biochemistry 30 (1991) 11147–11154.
[30] F.C. Almeida, S.J. Opella, fd coat protein structure in membrane environments: structural dynamics of the loop between the hydrophobic trans-membrane helix and the amphipathic in-plane helix, J. Mol. Biol. 270 (1997) 481–495.
[31] C.H. Papavoine, B.E. Christiaans, R.H. Folmer, R.N. Konings, C.W. Hilbers, Solution structure of the M13 major coat protein in detergent micelles: a basis for a model of phage assembly involving specific residues, J. Mol. Biol. 282 (1998) 401–419.
[32] K.A. Williams, N.A. Farrow, C.M. Deber, L.E. Kay, Structure and dynamics of bacteriophage IKe major coat protein in MPG micelles by solution NMR, Biochemistry 35 (1996) 5145–5157.
[33] K. Ikehara, H. Utiyama, M. Kurata, Studies on the structure of filamentous bacteriophage fd. II. All-or-none disassembly in guanidine-HCl and sodium dodecyl sulfate, Virology 66 (1975) 306–315.
[34] J. Griffith, M. Manning, K. Dunn, Filamentous bacteriophage contract into hollow spherical particles upon exposure to a chloroform-water interface, Cell 23 (1981) 747–753.
[35] M. Manning, S. Chrysogelos, J. Griffith, Mechanism of coliphage M13 contraction: intermediate structures trapped at low temperatures, J. Virol. 40 (1981) 912–919.
[36] D. Stopar, R.B. Spruijt, C.J. Wolfs, M.A. Hemminga, Mimicking initial interactions of bacteriophage M13 coat protein disassembly in model membrane systems, Biochemistry 37 (1998) 10181–10187.
[37] A.K. Dunker, L.D. Ensign, G.E. Arnold, L.M. Roberts, A model for fd phage penetration and assembly, FEBS Lett. 292 (1991) 271–274.
[38] J.S. Oh, D.R. Davies, J.D. Lawson, G.E. Arnold, A.K. Dunker, Isolation of chloroform-resistant mutants of filamentous phage: localization in models of phage structure, J. Mol. Biol. 287 (1999) 449–457.
[39] M. Manning, J. Griffith, Association of M13 I-forms and spheroids with lipid vesicles, Arch. Biochem. Biophys. 236 (1985) 297–303.
[40] L.M. Roberts, A.K. Dunker, Structural changes accompanying chloroform-induced contraction of the filamentous phage fd, Biochemistry 32 (1993) 10479–10488.
[41] K. Jacobsson, L. Frykberg, Phage display shot-gun cloning of ligand-binding domains of prokaryotic receptors approaches 100% correct clones, Biotechniques 20 (1996) 1070–1081.
[42] M. Russel, S. Kidd, M.R. Kelley, An improved filamentous helper phage for generating single-stranded plasmid DNA, Gene 45 (1986) 333–338.
[43] H. Khatoon, R.V. Iyer, V.N. Iyer, A new filamentous bacteriophage with sex-factor specificity, Virology 48 (1972) 145–155.
[44] P. Schwind, H. Kramer, A. Kremser, U. Ramsberger, I. Rasched, Subtilisin removes the surface layer of the phage fd coat, Eur. J. Biochem. 210 (1992) 431–436.
[45] L.A. Day, R.L. Wiseman, C.J. Marzec, Structure models for DNA in filamentous viruses with phosphates near the center, Nucleic Acids Res. 7 (1979) 1393–1403.
[46] S.A. Berkowitz, L.A. Day, Mass, length, composition and structure of the filamentous bacterial virus fd, J. Mol. Biol. 102 (1976) 531–547.
[47] J. Lakowicz, Principles of Fluorescence Spectroscopy, Plenum Press, New York, 1983.
[48] M.R. Eftink, C.A. Ghiron, Exposure of tryptophanyl residues and protein dynamics, Biochemistry 16 (1977) 5546–5551.
[49] R.W. Williams, A.K. Dunker, Circular dichroism studies of fd coat protein in membrane vesicles, J. Biol. Chem. 252 (1977) 6253–6255.
[50] Y. Nozaki, J.A. Reynolds, C. Tanford, Conformational states of a hydrophobic protein. The coat protein of fd bacteriophage, Biochemistry 17 (1978) 1239–1246.
[51] M. Manning, M. Moore, L. Spremulli, J. Griffith, Coat protein conformation in M13 filaments, I-forms and spheroids, Biochem. Biophys. Res. Commun. 112 (1983) 349–355.
[52] P. Luo, R.L. Baldwin, Mechanism of helix induction by trifluoroethanol: a framework for extrapolating the helix-forming properties of peptides from trifluoroethanol/water mixtures back to water, Biochemistry 36 (1997) 8413–8421.

[53] A. Gitter-Amir, K. Rosenheck, A.S. Schneider, Angular scattering analysis of the circular dichroism of biological cells. 1. The red blood cell membrane, Biochemistry 15 (1976) 3131–3137.
[54] E.M. Click, R.E. Webster, Filamentous phage infection: required interactions with the TolA protein, J. Bacteriol. 179 (1997) 6464–6471.
[55] J. Lubkowski, F. Hennecke, A. Plückthun, A. Wlodawer, The structural basis of phage display elucidated by the crystal structure of the N-terminal domains of g3p, Nature Struct. Biol. 5 (1998) 140–147.
[56] G. Glaser-Wuttke, J. Keppner, I. Rasched, Pore-forming properties of the adsorption protein of filamentous phage fd, Biochim. Biophys. Acta 985 (1989) 239–247.
[57] G. Böhm, R. Jaenicke, Correlation functions as a tool for protein modeling and structure analysis, Protein Sci. 1 (1992) 1269–1278.